Theor Chim Acta (1990) 77: 395–407

Theoretica Chimica Acta

Optical properties of perturbed NO_2^- ions in KNO_2 doped $NaNO_2$ single crystals

Carola Kryschi

Lehrstuhl für Festkörperspektroskopie (IPkM), Heinrich-Heine-Universität, D-4000 Düsseldorf, Federal Republic of Germany

Received January 8, 1990; received in revised form March 12, 1990/Accepted April 9, 1990

Summary. On the basis of high-resolution and time-resolved fluorescence spectra, a model is proposed for the interpretation of the fluorescence lines originating from various perturbed NO_2^- centers situated in the neighbourhood of the K^+ ion of the $NaNO_2:KNO_2$ crystal. Since their excited state energies are lower than that of the host, these perturbed NO_2^- ions act as traps for the host singlet exciton. On the assumption that the perturbation giving rise to those traps results from an interaction of the impurity ion K^+ with its nearest neighbours, the observed position of the energy levels of the various traps can be reconciled with crystal field calculations.

Key words: NO_2^- ions – KNO_2 doped $NaNO_2$ single crystals – Time-resolved fluorescence

1. Introduction

The high-resolution and time-resolved fluorescence spectra of $NaNO_2$ single crystals doped at 10^{-3} mole KNO_2/mole $NaNO_2$ have been reported in a series of papers [1–3]. In addition to the host spectrum, the fluorescence contains ten impurity-induced spectra which are attributed to ten distinct types of traps originating from perturbed NO_2^- ions in the direct and indirect neighbourhood of the impurity K^+ ion. The observed impurity-induced fluorescence intensities are about three orders of magnitude higher than the absolute dopant concentration suggests. It is generally accepted that this fluorescence occurs through nonradiative capture processes via deep defect traps. These capture processes allow the excitation energy to be transferred to the perturbed NO_2^- ions which act as the trap. The different traps can be classified into four deep traps, i.e., *A*, *F*, *G*, *N*, and six shallow traps, i.e., *B*, *C*, *D*, *I*, *J*, *K*. The depths of the deep traps lie in the region of 1000 cm^{-1}, whereas the depths of the shallow traps are less than 100 cm^{-1}.

In particular, there are three pairs of "cross-talking" traps consisting of one shallow and one deep trap, i.e., *B*-*A*, *C*-*F* and *D*-*G*. If the shallow trap is excited resonantly, the excitation energy will be transferred to one particular deep trap

of suitable spatial orientation. The absence of any interaction between the pairs of trap systems indicates that energy transfer takes place unidirectionally. Apparently the individual site geometry of the trapping NO_2^- ions determines its particular role in the interplay between the "communication" antennae.

In spite of intense experimental and theoretical research work on variously doped (e.g. with KNO_2, $AgNO_2$, $TeNO_2$, $Pb(NO_2)_2$) $NaNO_2$ single crystals in the past [4–9], the nature of impurity-induced traps is still only roughly understood. So far the respective trap-fluorescence spectra could not be assigned to distinctly perturbed NO_2^- ions because the individual site geometries of the trapping NO_2^- ions were unknown.

In the present paper we focus our attention on the point defect distortions of the four deep traps *A*, *N*, *F*, *G* whose individual fluorescence spectra have been identified recently by resonant excitation [3]. On the basis of spectroscopic data such as trap depths, vibrational frequencies and relative line intensities, we provide a rationalization for the trap fluorescence spectra considering the respective location of each deep trap in geometric relation to the impurity K^+ ion. Employing ligand-field theory [10, 11], we calculate the shift of the fluorescence origin in the trapping sites relative to that of the unperturbed host NO_2^- molecules, so as to reveal the static structural distortions of the environment of the distinct traps due to the presence of the K^+ ion. On the basis of this theoretical treatment we will correlate the experimentallly obtained trap depths to distinct distorted NO_2^- ions in the direct neighbourhood of the K^+ ion. Furthermore, we will relate some of the above conclusions with those derived from fluorescence lifetimes by taking into account the distortional effect on molecular geometry of the trap NO_2^- ions.

2. Theoretical analysis

2.1. Crystal properties

In the ferroelectric phase (i.e. below 163°C) the $NaNO_2$ crystal structure is orthorhombic C_{2v}^{20} body centered with two translationally equivalent formula units per primitive cell [12]. The lattice constants are $a = 0.3568$ nm, $b = 0.5576$ nm and $c = 0.5392$ nm [13]. The site symmetry of the NO_2^- ions is C_{2v}. The O–N–O bond forms an angle of $\beta = 115.6°$. The NO_2^- ions are lined up in the *bc* plane so that their transition dipole moments are directed along the *a* axis. In KNO_2 doped $NaNO_2$ crystals the impurity K^+ ion occupies a host Na^+ site. Thus, each K^+ ion resides at a site of C_{2v} symmetry surrounded by a distorted octahedron of NO_2^- ions.

2.2. Nature of fluorescence transition

The fluorescence spectra of the host NO_2^- ion and of the four trap NO_2^- ions under consideration consist of long progressions built on the totally symmetric bending vibration ν_2 of the NO_2^- molecule. Additionally, one quantum of the totally symmetric stretching vibration ν_1 is seen, partially superimposed by the phonon side bands of the ν_2 lines (see Fig. 1a). The vibrational frequencies of the

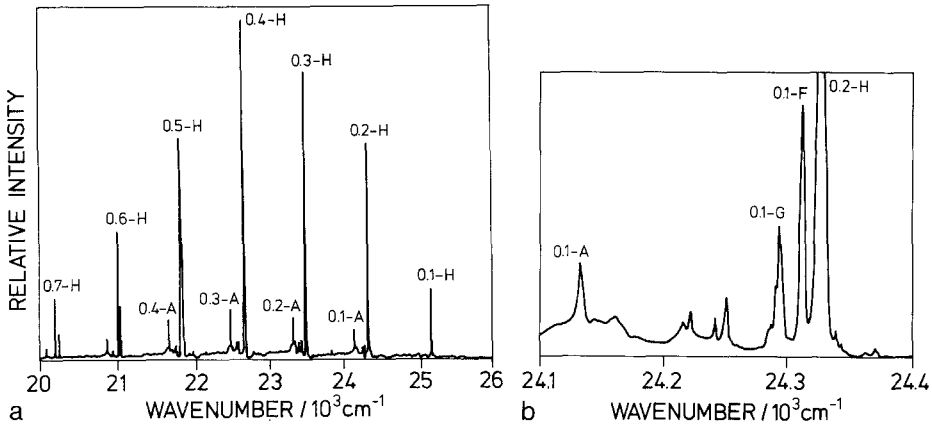

Fig. 1. **a** The overall fluorescence spectra of KNO_2 doped $NaNO_2$ at 4.2 K from [1]. **b** The *A*, *F* and *G* trap fluorescence lines in the neighbourhood of the 0.2-H (host) line of the fluorescence spectrum of $NaNO_2$ doped with 0.14% KNO_2 at 4.2 K [3]; the *N* trap fluorescence lines are too weak in any spectral range to be detected in the neighbourhood of the host lines [3]

Table 1. Spectroscopic data [3] and calculated valence-angle differences for the host molecule and for the four deep trap NO_2^- ions at 4.2 K

	ν_{00} (cm^{-1})	ν_1 (cm^{-1})	ν_2 (cm^{-1})	ν_2^* (cm^{-1})	$\Delta\alpha$ (°)	τ (ns)
Host	25980	1325	829	630	9.4°	8.2
A	24949	1340	817	634	8.60	7.6
F	25127	1317	816	631	8.36	7.4
G	25103	1331	811	635	8.02	34.0
N	25490	–	822	–	8.76	8.0

host molecules are $\nu_2 = 829\ cm^{-1}$ and $\nu_1 = 1325\ cm^{-1}$. In the trap spectra both the ν_1 and ν_2 frequencies are slightly different from all of the unperturbed host molecules (see Table 1). In the case of the host spectrum the maximum intensity is at the fourth member in the ν_2 progression, whereas in the *G*, *N* and *F* trap spectra the third member is the dominant one. The *A* trap spectrum shows a maximum intensity at the second member.

Calculating the spectral fluorescence intensity distribution for the pure $NaNO_2$ crystal, Kokai and Azumi [14] determined a bond-angle difference between excited and ground state NO_2^- ion of $9.6 \pm 0.4°$. Applying a comparable computational procedure [15] to the intensity distribution of the host-fluorescence spectrum, we have obtained a very similar result of $9.4 \pm 0.3°$; the N–O bond length is changed insignificantly by an amount of 0.06 Å. Concerning the trap-fluorescence spectra, the calculated bond-angle changes are smaller by 0.7 to 1.4° (see Table 1) and in contrast to the host, a small contribution due to mode mixing (Duschinsky-rotation angle $\alpha \approx 1.5$–4°) could be found. The distortions due to the K^+ impurity ion may affect the molecular geometry of the trap NO_2^-

ions. The ν_2 bending mode frequencies of the trap NO_2^- considered here—ranging between 811 cm^{-1} and 822 cm^{-1}—are significantly smaller than the frequency $\nu_2 = 829\ cm^{-1}$ of the host NO_2^-. In accordance with recent molecular orbital geometry calculations [16], the decrease of the bending mode frequency is related to the increase of the bond angle. The larger ground-state bond angles are due the more polarizable K^+ ion attracting the electron in the antibonding $6a_1$ molecular orbital of NO_2^-. In the terms of Walsh rules [17] complete removal of the electron in the antibonding MO will yield an increase of the bond angle of about 15°. Since reabsorption events cause the O–O fluorescence transition to disappear from the emission spectra, the absolute trap depths have been established by means of fluorescence excitation spectra. Table 1 summarizes the experimental fluorescence spectroscopic data and the calculated bond-angle differences between the ground state and excited state.

2.3. Geometric assignment of the deep traps

Figure 2 displays the unit cell of the $NaNO_2$ crystal with the NO_2^- ions in the direct and indirect vicinity of a K^+ ion positioned in the cell. When considering the six nearest-neighbour NO_2^- ions surrounding the K^+ impurity, there are three distinct traps. The *A* trap, representing the most strongly distorted NO_2^- ions with respect to the site symmetry, is assigned to one of the four energetically equivalent NO_2^- ions in the *ac* plane roughly containing K^+. Since K^+ has a larger size than the Na^+ ion, these four NO_2^- ions around the *A* trap are pushed along the directions $(-1, 1, 1), (1, 1, 1), (-1, 1, -1), (1, 1, -1)$, respectively.

The *N* trap is supposed to occupy the site located next to the K^+ impurity ion which resides along the bisector of the ONO angle. We derive this assignment from the striking absence of any energy transfer occurring either via a shallow trap or directly via the host. This NO_2^- ion is strongly exposed to the K^+ ion whose shielding effect inhibits energy-transfer processes from any other NO_2^- ion. Moreover, the ground-state bending vibrational frequency $\nu_2 = 822\ cm^{-1}$ is comparable with that of the host molecule, indicating a high degree of symmetry of this displacement.

The *G* trap is assigned to the NO_2^- ion on the other side of the K^+ ion along the *b* axis. The distorted ligand field potential around the *G* trap arises from a the superposition of the direct displacement of the central ion due to the presence of the heavier K^+ ion and the displacement of the *A*-trap NO_2^- ions.

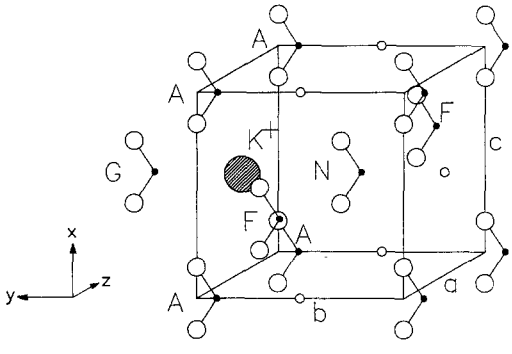

Fig. 2. The unit cell of $NaNO_2$ containing a K^+ ion. The four traps *A*, *F*, *N* and *G* are indicated. ◍, Potassium; ●, nitrogen; ○, oxygen; ○, sodium

The F trap is located in front of and behind the N trap when viewing along the a axis. The perturbation considered here arises from the interaction of the K^+ ion with the F-trap and two A-trap NO_2^- ions. Consequently, the F-trap NO_2^- ion experiences a displacement in the (0, −1, 1) or (0, −1, −1) direction, whereas the A-trap NO_2^- ions are displaced in the (1, 1, 1) and (−1, 1, 1) or (1, 1, −1) and (−1, 1, −1) directions.

2.4. *Static perturbation*

In order to evaluate the trap depths we use the ligand field theory to derive the potential associated with the force acting on the valence electrons of the central NO_2^- ion for the trap considered

$$V = \sum_{1}^{\infty} \sum_{\lambda=l}^{-l} A_{l,\lambda} \sum_{i=1}^{n} r_i^l Y_l^{\lambda}(\theta_i, \phi_i), \tag{1}$$

where

$$A_{l,\lambda} = -[4\pi/(2l+1)]\, q_k \sum_{k=1}^{n} (1/R_k^{l+1}) Y_l^{\lambda *}(\Theta_k, \Phi_k). \tag{2}$$

The index i labels the electrons of the trap under consideration, taken as a central NO_2^- ion, and the index k the nearest-neighbour ligands Na^+ and NO_2^- in the first and second coordination shells. R_k is the distance between the kth ligand (treated as a point charge) and the central ion and, r_i represents the radial coordinate of the ith valence electron from the mass center of the central ion. q_k in Eq. (2) is the effective point charge of the ligands and Y_l^{λ} is spherical harmonic of rank l. In the forthcoming the spherical coordinates θ and ϕ of the electrons are omitted (i.e. $Y_l^{\lambda} \equiv Y_l^{\lambda}(\theta, \phi)$).

It is convenient for each trap to split the ligand field V into

$$V_t = V_c + \Delta V_t, \qquad t = A, F, G, N, \tag{3}$$

i.e., the electrons associated with the central NO_2^- ion are subjected to the fields ΔV_t in addition to the unperturbed field V_c. The latter is associated with the undoped crystal and thus has C_{2v} symmetry. It is of the form

$$\begin{aligned} V_c = {} & 2\,(\pi/10)^{1/2} \{8\,(2\cos^2\Theta - \sin^2\Theta)\; 1/R^3 \\ & - [4\,(2\cos^2\Theta' - \sin^2\Theta')\; 1/R'^3 + 2/R''^3]\}|q|\, r^2\, Y_2^0 \\ & + (3\pi/5)^{1/2}\,(4/R'^3 - 2/R''^3)|q|\, r^2\,(Y_2^2 + Y_2^{-2}) + \cdots, \end{aligned} \tag{4}$$

where R' and R'' denote the respective distances between the central ion and the Na^+ ions in the first coordination sphere; R indicates the distance between the central ion and the NO_2^- ions in the second coordination sphere, i.e. $R' = 0.3237$ nm, $R'' = 0.2879$ nm and $R = 0.4269$ nm. The angles Θ and Θ' stand for the corresponding angular coordinates with $\Theta' = 56.21°$ and $\Theta = 57.39°$. The effective point charges are $q(Na^+) = +|q|$ and $q(NO_2^-) = -|q|$.

On the other hand, the contribution ΔV_t in Eq. (3) arises from the static distortion in the neighbourhood of the trap t. The potential ΔV_t may be obtained by differentiating the ligand field potential V with respect to the cartesian displacements $a_1, b_1, c_1, \ldots, a_n, b_n, c_n$ of the surrounding ligands, giving an expansion only up to terms linear in the ligand displacements. This leads to an

expression similar to that of Eq. (1):

$$\Delta V_t = \sum_{1}^{\infty} \sum_{\lambda=l}^{-l} \bar{A}_{l,\lambda} \sum_{i=1}^{n} r_i^l Y_l^{\lambda}(\theta_i, \phi_i), \tag{5}$$

with

$$\bar{A}_{l,\lambda} = -[4\pi/(2l+1)]\, q_k \sum_{k=1}^{n} [(a_k\, \partial/\partial x_k + b_k\, \partial/\partial y_k + c_k\, \partial/\partial z_k) \times Y_l^{\lambda *}(\Theta_k, \Phi_k)/(R_k^{l+1})]_{eq}, \qquad t = A, F, G, N \tag{6}$$

where $x_1, y_1, z_1, \ldots, x_n, y_n, z_n$ represent $3n$ components of a unit vector transformed from the corresponding spherical coordinates R_k, Θ_k, Φ_k ($k = 1, 2, \ldots, 8$). This transformation is performed in the usual way, viz.

$$x_k = x_k^0 + R_k \sin \Theta_k \cos \Phi_k,$$
$$y_k = y_k^0 + R_k \sin \Theta_k \sin \Phi_k,$$
$$z_k = z_k^0 + R_k \cos \Theta_k,$$

where x_k, y_k, z_k and x_k^0, y_k^0, z_k^0 denote the cartesian coordinates of the distorted and equilibrium ligand positions. The derivatives in Eq. (6) thus become

$$\partial/\partial x_k = \partial/\partial R_k \cdot \partial R_k/\partial x_k + \partial/\partial \Theta_k \cdot \partial \Theta_k/\partial x_k + \partial/\partial \Phi_k \cdot \partial \Phi_k/\partial x_k, \tag{7}$$

and similar relations hold for $\partial/\partial y_k$ and $\partial/\partial z_k$. It can be shown by group theory arguments that the quantity $\bar{A}_{l,\lambda}$ is independent of the index λ representing the subrepresentation of l (see Eq. (4) in [11]). For the displacement of the central ion, which coordinates x_0, y_0 and z_0 are not contained in the potential V, the calculation of the coefficients $\bar{A}_{l,\lambda}$ and hence of the corresponding contribution to ΔV_t may be performed by leaving the position of the central ion unchanged and displacing the peripheral ligands numbered k over a distance $x_k = -x_0$, $y_k = -y_0$ or $z_k = z_0$. This follows from the fact that

$$(\Sigma_k\, \partial/\partial x_k - \partial/\partial x_0) V = 0, \tag{8}$$

since $-x_0$ and all x_k displacements leave the ligand field operator invariant. Equations similar to (8) hold for the y and z components also.

2.5. Term shifts

By means of the perturbation potential V_t we evaluate the changes in the ground state and excited state energies and take the differences ΔE_t ($t = A, F, N, G$). If Ψ^{1A_1} and Ψ^{1B_1} are the molecular wave function of the ground $^1A_1$ and excited $^1B_1$ state, respectively, we have

$$\Delta E_t = \langle \Psi^{1B_1} | \Delta V_t | \Psi^{1B_1} \rangle - \langle \Psi^{1A_1} | \Delta V_t | \Psi^{1A_1} \rangle. \tag{9}$$

Note that the operator ΔV_t consists of a set one-electron operators. Then if the molecular wave functions Ψ^{1A_1} and Ψ^{1B_1} are represented by their Slater determinants built on the valence MOs, the matrix elements in Eq. (9) can be reduced on the molecular orbital level to give [18]

$$\Delta E_t = \langle \varphi_{n\mathrm{N}} | \Delta V_t | \varphi_{n\mathrm{N}} \rangle - \langle \varphi_{\pi^*} | \Delta V_t | \varphi_{\pi^*} \rangle, \tag{10}$$

where $\varphi_{n\mathrm{N}}$ and φ_{π^*} are the LUMO and HOMO of the central NO_2^- ion. The

latter are represented by the linear combination of valence atomic orbitals [19]:

$$\varphi_{n\mathrm{N}} = 0.355\,\chi_{2s}(\mathrm{N}) - 0.736\,\chi_{px}(\mathrm{N}) - 0.011\,\{\chi_{2s}(\mathrm{O}_1) + \chi_{2s}(\mathrm{O}_2)\}$$
$$- 0.016\,\{\chi_{py}(\mathrm{O}_1) - \chi_{py}(\mathrm{O}_2)\} + 0.491\,\{\chi_{px}(\mathrm{O}_1) + \chi_{px}(\mathrm{O}_2)\} \qquad (11)$$
$$\varphi_{\pi^*} = 0.948\,\chi_{pz}(\mathrm{N}) - 0.437\,\{\chi_{pz}(\mathrm{O}_1) + \chi_{pz}(\mathrm{O}_2)\},$$

where $\chi(\ )$ denote the $2s$ and $2p$ orbitals of the nitrogen and oxygens. The HOMO $\varphi_{n\mathrm{N}}$ is a lone pair orbital, whereas the LUMO φ_{π^*} is an antibonding π orbital. The first one is largely localized on the nitrogen atom. From Eqs. (9) and (10) it is evident that the energy shift and thereby the stabilization of the states $\Psi^{1}A_1$ and $\Psi^{1}B_1$ occur for those components of ΔV_t which transform according to the totally symmetric representation of the C_{2v} group of the crystallographic unit cell.

3. Results and discussion

3.1. Derivation of the static distorted potential field of the N, A, F and G traps

Turning first to the N trap, we have a situation where the central NO_2^- ion (i.e., the N trap) is pushed by the K^+ ion along the b axis over a distance $-y_N$. Since the coordinate y_N is not contained in the potential V, the ligand field potential ΔV_N associated with the force acting on any one of the valence electrons of the central ion is calculated by means of Eq. (8), i.e. by leaving the position of the central ion unchanged and displacing the nearest-neighbour ligands over a distance $y_k = -y_N$. The nearest-neighbour ligands are the five Na^+ ions in the first, and the eight NO_2^- ions in the second coordination spheres. Their displacement is represented by the arrows given in Fig. 3 which indicate the direction and the magnitude of the ligand motion. Other perturbations of the ligand field arising from interactions of the K^+ ion and its neighbouring NO_2^- ions are assumed to be negligibly small because of the shielding effect of the K^+ ion on the N-trap NO_2^- ion. Making use of Eqs. (5)–(7) we obtain ΔV_N as a function of the coordinates of the valence electrons

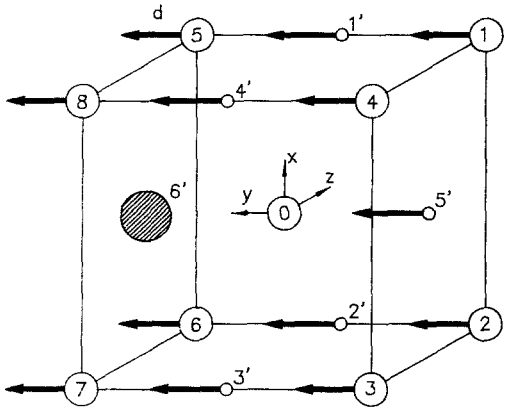

Fig. 3. Static local site distortion due to the presence of K^+ ion in the unit cell corresponding to the N trap. The measure of this distortion is the (complementary) displacement d of the first and second coordination shell of the N trap, where the C_{2v} symmetric displacements of the surrounding ligands Na^+ (first coordination shell) and NO_2^- (second coordination shell). ◍, K^+; ○, NO_2^-; ○, Na^+

of the N-trap ion:

$$\Delta V_N = d\,\{8(\pi/6)^{1/2}\cdot[(2\sin^2\Theta-\cos^2\Theta-1)(1/R^3)$$
$$+(1/R'^3-1/2R''^3)]|q|r\,i\,(Y_1^1+Y_1^{-1})$$
$$+3\,(\pi/5)^{1/2}(1/R''^4)|q|\,r^2Y_2^0+(3\pi/10)^{1/2}(1/R''^4)|q|\,r^2(Y_2^2+Y_2^{-2})\}, \quad (12)$$

where $\Theta = 57.386°$, $q(NO_2^-) = -|q|$ and $q(Na^+) = +|q|$. It is convenient to calculate expressions like (12) in atomic units, thus $R = 8.0673\,a_0$, $R' = 6.1173\,a_0$ and $R'' = 5.4409\,a_0$. The parameter d is a measure of the distortion. Since for the system under consideration spherical harmonics of rank $l > 2$ do not contribute to the energy shift, we terminate the expansion after terms for which $l \leqslant 2$. For the sake of simplicity, the b and c axes of the unit cell have been assumed to be equal.

In the case of the A trap the K^+ ion is thought to occupy the site of one of the Na^+ ions 1′, 2′, 3′ or 4′, thus destroying the C_{2v} symmetry of the unit cell (see Fig. 4). On the other hand, the A-trap ion is pushed by the K^+ ion spatial-diagonally, which leads to displacements of the ligands along the a, b, and c axes. Since only the y component of these displacements exhibits C_{2v} symmetry, the considered ligand field ΔV_A is derived by displacing the eight NO_2^- ions as well as the Na^+ ions 5′ and 6′ in the planes $y = 0$ and $y = b$ by the amount $-e\sum_{k=1}^{8} y_k(NO_2^-) - e\sum_{k=5'}^{6'} y_k(Na^+)$. This yields

$$\Delta V_A = e\,\{8\,(\pi/6)^{1/2}[(-2\sin^2\Theta+\cos^2\Theta+1)(r/R^3)+(r/R''^3)]|q|\,i\,(y_1^1+y_1^{-1})\}. \quad (13)$$

The G trap possesses the A traps as ligands. The displacements of the latter are $e\,(x_1-x_2-x_3+x_4, y_1+y_2+y_3+y_4, z_1+z_2-z_3-z_4)$ with e denoting the relative length of the distortion (see Fig. 5). These are superimposed on the compensating displacements for the central ion

$$g\left\{\sum_{k=1}^{8} y_k(NO_2^-)+\sum_{k=1'}^{6'} y_k(Na^+)\right\}.$$

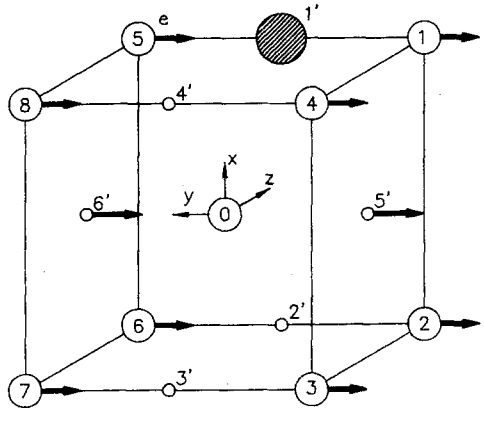

Fig. 4. Static local site distortion in the vicinity of the A-trap center. The relative motion of the ligands are represented by arrows that indicate both the direction and the relative length e of the distortion; only the totally symmetric component has been retained. Symbols as for Fig. 3

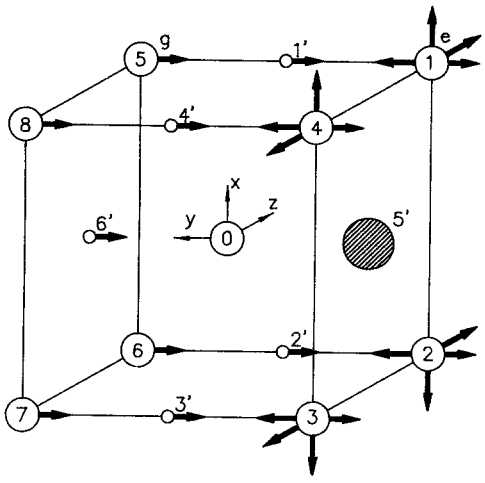

Fig. 5. Static local site distortion of the *G*-trap center inside the first and second coordination shells. Only the totally symmetric (C_{2v}) component of the distortion is taken. Symbols as for Fig. 3

Thus, the corresponding potential change is

$$\begin{aligned}\Delta V_G = g\,\{&8\,(\pi/6)^{1/2}[(-2\sin^2\Theta+\cos^2\Theta+1)(r/R^3)\\&-((r/R'^3)-(r/2R''^3))]|q|\,i\,(Y_1^1+Y_1^{-1})\\&-3\,(\pi/5)^{1/2}(r^2/R''^4)|q|Y_2^0\\&-3\,(3\pi/10)^{1/2}(r^2/R''^4)|q|(Y_2^2+Y_2^{-2})\}\\&+e\,\{4\,(\pi/6)^{1/2}(4\sin^2\Theta+3\sqrt{2}\cos\Theta\sin\Theta)(r/R^4)|q|\,i\,(Y_1^1+Y_1^{-1})\\&+4\,(\pi/10)^{1/2}(-12\sin\Theta\cos^2\Theta\\&-\sqrt{2}\,(6\cos^3\Theta-9\sin^2\Theta\cos\Theta))(r^2/R^4)|q|\,Y_2^0\},\end{aligned}\tag{14}$$

with $e<g$ and $d>e$. d, e and g denote the relative length of the distortions.

The F trap is located both in front of and behind the N-NO_2^- ion. In regard to the one in front of the N trap, the main component of the direct displacements of the NO_2^- ions 7, 8 due to the K^+ is directed along the a axis (see Fig. 6). On the other hand, the F trap is shifted slightly along the direction (0, −1, 1), so that the resulting displacements arise from the superposition of both. Additionally, the Na^+ ion 6′ is pushed along the a axis and degrades the C_{2v} symmetry of the first coordination shell. Hence, the contributing displacements of the Na^+ ions 1′, 2′, 3′, 4′ and of the NO_2^- ions are $f\{\sum_{k=1}^{8} y_k(NO_2^-)+\sum_{k=1'}^{4'} y_k(Na^+)\}$ superimposed on $f\{z_5+z_6+z_7-z_8\}$. Thus we obtain

$$\begin{aligned}\Delta V_F = f\,\{&8\,(\pi/6)^{1/2}[(2\sin^2\Theta-\cos^2\Theta-1)(r/R^3)\\&+(3\sqrt{2}\cos\Theta\sin\Theta)(r/2R^3)+(r/R'^3)]|q|\,i\,(Y_1^1+Y_1^{-1})\\&-(\pi/5)^{1/2}[(6\cos^3\Theta-9\cos\Theta\sin^2\Theta)(2/R^4)]|q|r^2Y_2^0\},\end{aligned}\tag{15}$$

where f denotes the relative length of the distortion.

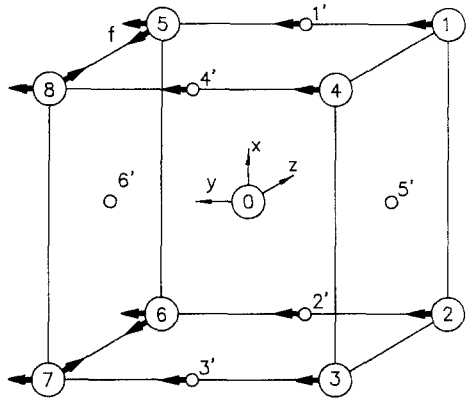

Fig. 6. Static local site distortion around the *F*-trap radiating center, including the first and second coordination shells. Only the totally symmetric component of the distortion is taken. Symbols as for Fig. 3

3.2. Evaluation of the trap depth

Inserting the expressions (11) for $\varphi_{n\mathrm{N}}$ and φ_{π^*} in Eq. (10) and using the tables in [20] to calculate the angular part of the integrals in Eq. (10) we obtain, after lengthy calculations, the energy differences ΔE_t of the individual traps

$$\Delta E_{N(\mathrm{calc.})} = -d\,\{1.821 \times 10^{-3}\langle A(r)\rangle + 8.053 \times 10^{-5}\langle B(r)\rangle\}$$

$$\Delta E_{A(\mathrm{calc.})} = -e\ 7.197 \times 10^{-3}\langle A(r)\rangle$$

$$\Delta E_{G(\mathrm{calc.})} = g\,\{1.820 \times 10^{-3}\langle A(r)\rangle + 8.053 \times 10^{-5}\langle B(r)\rangle\} - e\,\{5.475 \times 10^{-3}\langle A(r)\rangle + 3.886 \times 10^{-4}\langle B(r)\rangle\}$$

$$\Delta E_{F(\mathrm{calc.})} = -f\,\{7.780 \times 10^{-3}\langle A(r)\rangle - 1.318 \times 10^{-4}\langle B(r)\rangle\}, \qquad (16)$$

where the abbreviations $\langle A(r)\rangle = |q|\langle r\rangle$ and $\langle B(r)\rangle = |q|\langle r^2\rangle$ have been used; $\langle r\rangle$ and $\langle r^2\rangle$ represent the averages of r and r^2 with respect to the radial part of $\varphi_{n\mathrm{N}}$ and φ_{π^*} over the whole central ion charge distribution (for definition of $\langle r^n\rangle$ see for example [10] and [20]).

The value of $\langle B(r)\rangle$ is calculated by means of the expression of the unperturbed ligand field potential V_c in Eq. (4). Using a similar relation to that of Eq. (10) for V_c, the crystal shift ΔE_c for the undoped $NaNO_2$ becomes

$$\Delta E_c = -1.4468 \times 10^{-3}\langle B(r)\rangle. \qquad (17)$$

In order to determine ΔE_c, the pure electronic absorption transition of the free NO_2^- ion has been determined from *ab initio* calculations, yielding $\Delta E_{\mathrm{ion}} = 0.1264$ au [21]. Using the relation $\Delta E_c = \Delta E_{\mathrm{ion}} - \Delta E_{\mathrm{host}}$, where $\Delta E_{\mathrm{host}} = \nu_{00}$ (host) is known from experiment (see table 1), we obtain $\langle B(r)\rangle = 5.588$ au from Eq. (17). The value of $\langle A(r)\rangle$ is calculated by means of the relationship $\langle A(r)\rangle = \langle B(r)\rangle \cdot \langle r^2\rangle/\langle r\rangle = 3.164$ au, where the values of $\langle r\rangle$ and $\langle r^2\rangle$ are obtained by using the SCF function for N of Clementi [22]: $\langle r\rangle = 2.898\ a_0$, $\langle r^2\rangle = 5.118\ a_0^2$. Using the value for $\langle B(r)\rangle$, $|q|$ becomes then 1.08 e which is a very likely value for $|q|$.

Since the molecular wave functions of the ground and excited singlet states are mainly localized on the nitrogen atom, the matrix elements in Eq. (10) have been approximated by one-center matrix elements involving the nitrogen. In order to justify this approximation the contribution due to the oxygen atoms have been estimated for $\varphi_{n\mathrm{N}}$ (see Eq. (11)) by calculting three-center matrix elements which contain the nitrogen $2s$ AO and the two oxygen $2p_x$ AOs. Using a system of coordinates as in [23] we obtain values of these three-center matrix elements which are smaller than 5% of the corresponding one-center matrix elements.

The absolute trap depths are known from experiment (see Table 1),

$$\Delta E_N = 2.233 \times 10^{-3}\ \text{au}, \qquad \Delta E_A = 4.698 \times 10^{-3}\ \text{au},$$

$$\Delta E_G = 3.996 \times 10^{-3}\ \text{au}, \qquad \Delta E_F = 3.887 \times 10^{-3}\ \text{au},$$

and so it is now straightforwrd to solve the system of four equations (16) with respect to the values of the ligand displacements. The result is

$$\begin{aligned} d &= 0.360\, a_0, \qquad e = 0.206\, a_0, \\ g &= 0.005\, a_0, \qquad f = 0.163\, a_0. \end{aligned} \tag{18}$$

These values are sufficiently small to justify the method used, i.e. treating the distortion experienced by each trap t due to the neighbouring K^+ impurity as a perturbation ΔV_t to the unperturbed field V_c. The largest displacement d is roughly 6% of the shortest distance between central ion and ligands which is $R'' = 5.4409\, a_0$. Moreover, the relative magnitudes of the geometric distortions in the $NaNO_2$ crystal (depicted in Figs. 3–6) which are given by Eqs. (18) confirm the suggested assignments of the impurity-induced fluorescence spectra (i.e. the traps A, F, G and N) to distinct distorted NO_2^- ions in the direct neighbourhood of the impurity K^+.

3.3. Radiative lifetimes of A, F, N and G traps

The time-resolved fluorescence experiments yield a radiative lifetime τ of about 8 ns for three traps A, F and N, which is similar to that in the undoped $NaNO_2$ lattice (see Table 1). On the contrary, the fluorescence lifetime of the G trap is increased by a factor of 4. The reason for the long lifetime is due to the Duschinsky mixing effect strongly affecting the Franck–Condon factor [12], which in turn is responsible for the fluorescence intensity. In comparison with the other traps, the bending mode of the G trap fluorescence has the lowest frequency, $\nu_2 = 811\ \text{cm}^{-1}$, and consequently the largest ground-state bond angle. As mentioned above (see Sect. 2.2) this is due to the neighbouring K^+ ion affecting the electron density of the antibonding $6a_1$ MO of NO_2^-. The changes in the electron distribution and ground-state geometry can possibly cause a mixing of the bending and stretching modes (Duschinsky-rotating angle $\alpha = 4°$). If the mixing of the bending and stretching modes is negligibly small, the stretching mode participates very weakly in the fluorescence transition. In the case of efficient mixing, the overlap integrals for the vibrational wavefunctions involving both the bending and the stretching mode are such that they tend to force the molecular ion to fluoresce at a lower frequency than those of non-

mixed modes [24]. Following the argument of Douglas [24] this frequency effect causes an increase of the fluorescence lifetime, since the latter is reciprocally proportional to the cube of the frequency.

4. Conclusions

In this paper an attempt has been made to correlate the observed trap fluorescence of distorted NO_2^- ions in $NaNO_2:KNO_2$ with a theoretical calculation based on the static local site distortion due to the K^+ ion. On the basis of this correlation the experimentally obtained trap depths have been assigned to distinct distorted NO_2^- ions in the direct environment of K^+. These results were obtained by considering a model where the trap NO_2^- ion experiences a change in the electrostatic potential because of the displacements of the point-charge nearest neighbours. The latter consist of all Na^+ ions in the first coordination sphere and the eight NO_2^- in the second coordination sphere around the trap NO_2^- ion. In order to account for the static local site distortion the electrostatic potential has been expanded up to linear terms in the displacement coordinates of the nearest neighbours by assuming the latter are point-charges. By means of this potential field, the energetic shifts of the states of the distorted NO_2^- ions which act as traps for the host exciton have been calculated.

It would be wrong, however, to conclude from this alone that a local short range perturbation of the nearest neighbours applies for excited radiating centers in general. In the special case of $NaNO_2:KNO_2$, the trap fluorescence is strongly localized and resembles that of the free NO_2^- ion fluorescence. This is due to the fact that, on the one hand, the width of the host exciton band is smaller than $10\,cm^{-1}$ [2] and on the other hand, the relevant trap depths are larger than $400\,cm^{-1}$. The observed common frequency intervals and the well-defined structure suggest that the side bands correspond to local modes of vibrations of a NO_2^- center rather than to lattice modes. Since the frequencies and linewidths of the host-absorption as well as fluorescence lines coincide totally with the corresponding spectra of pure $NaNO_2$ crystal, the distortions due to the K^+ impurity are very likely to be limited to the direct environment. These facts strongly support the assumption of the localized nature of the traps and of their limiting treatment by taking into account only two coordination spheres of their nearest neighbours.

Acknowledgements. The author would like to thank Dr. H. Kupka for many very instructive as well as stimulating discussions, and Prof. Dr. D. Schmid for his deep interest and support. The author is also indebted to Dr. Th. Schmidt and J. Köhler for motivating this paper with their intense experimental work.

References

1. Lisse F, Köhler J, Pufahl H, Schmid D (1987) phys stat sol (b) 140:605
2. Pufahl H, Köhler J, Schmidt Th, Schmid D, Kenkre VM (1987) phys stat sol (b) 141:303
3. Schmidt Th, Köhler J, Kryschi C, Schmid D (1988) phys stat sol (b) 147:797
4. Dietrich W, Schmid D (1976) phys stat sol (b) 74:609
5. Hochstrasser RM, Marchetti AP (1969) Chem Phys 50:1727
6. Dietrich W, Drissler F, Schmid D (1977) Chem Phys Lett 51:413

7. Reznik LE (1986) phys stat sol (b) 136:417
8. Clark SE, Tinti DS (1979) Chem Phys Lett 60:292
9. Clark SE, Tinti DS (1980) Chem Phys 51:17
10. Ballhausen CJ (1979) Molecular electronic structure of transition metal complexes. McGraw-Hill, New York
11. Kupka H, Wernicke R, Ensslin W, Schmidtke H-H (1979) Theor Chim Acta 51:297
12. Kay MI (1972) Ferroelectrics 4:235
13. Kucharczyk D, Pietraszko A, Tukaszewicz K (1976) phys stat sol (a) 37:287
14. Kokai F, Azumi T (1982) J Phys Chem 86:179
15. Kupka H, Polansky OE (1984) J Chem Phys 80:3153
16. Ervin KM, Ho J, Linneberger WC (1988) J Phys Chem 92:5405
17. Buenker RJ, Peyerimhoff SD (1974) Chem Rev 74:127
18. Slater JC (1960) Quantum theory of atomic structure, vol. I. McGraw-Hill, New York
19. Kato H, Yonezawa T, Morokuma K, Fukui K (1964) Bull Chem Soc Jap 37:1710
20. Sugano S, Tanabe Y, Kamimura H (1970) Multiplets of transition-metal ions in crystal. Academic Press, New York
21. Handy NC, Goddard JD, Schäfer III HF (1979) J Chem Phys 71:426
22. Clementi E (1965) IBM J Res Develop 9:2
23. Kuppermann A, Karplus M, Isaacson LM (1959) Z Naturforschg 14a:311
24. Douglas AE (1966) J Chem Phys 45:1007